J. Electrochem. Sci. Eng. **16** (2026) 3048; https://doi.org/10.5599/jese.3048

Open Access : : ISSN 1847-9286
https://pub.iapchem.org/ojs/index.php/JESE

Original scientific paper

Development of a modified electrode using magnesium ferrite/activated carbon from coffee shell for determination of paracetamol

Phan Thi Kim Thu[1], Phan Tu Quy[1], Nguyen Mau Thanh[2], Nguyen Quang Man[3], Nguyen Hai Phong[4] and Dinh Quang Khieu[4,✉]

[1]*Tay Nguyen University, 630000, Vietnam*
[2]*Quang Binh University, 510000, Vietnam*
[3]*University of Medicine and Pharmacy, Hue University, 530000, Vietnam*
[4]*University of Sciences, Hue University, 530000, Vietnam*

Corresponding Author: ✉dqkhieu@hueuni.edu.vn

Received: October 12, 2025; Accepted: December 27, 2025; Published: January 1, 2026

Abstract

This study aimed to develop a simple and effective electrochemical sensor for detecting paracetamol (PAR) in pharmaceutical tablets. The goal was to synthesize and utilize a novel nanocomposite of magnesium ferrite, $MgFe_2O_4$, and activated carbon derived from coffee shells (MF/AC) as a high-performance electrode modifier. The MF/AC nanocomposite was produced using a hydrothermal method. It was characterized with techniques such as scanning electron microscopy, Fourier transform infrared spectroscopy, X-ray diffraction, energy-dispersive X-ray spectroscopy, nitrogen adsorption/desorption, Raman spectroscopy and a vibrating sample magnetometer. The electrochemical activity of the MF/AC-modified glassy carbon electrode (MF/AC--GCE) for PAR oxidation was evaluated by cyclic voltammetry and differential pulse voltammetry, with parameters such as scan rate and pH examined. The optimized sensor demonstrated excellent performance with two linear detection ranges for PAR: 1.0 to 9.9 µM (R^2 = 0.999), and 9.9 to 47.62 µM (R^2 = 0.999), with a low detection limit of 0.29 µM. The method was successfully applied to analyse five commercial pharmaceutical products, showing high accuracy, acceptable recovery rates, and strong agreement with High-performance liquid chromatography validation results. The developed MF/AC-GCE sensor provides a simple, effective, and environmentally friendly approach for the electrochemical detection of paracetamol. Its impressive performance suggests potential applications in pharmaceutical quality control and clinical diagnostics, offering a practical alternative to more complex analytical techniques.

Keywords
Electrochemical sensor; nanocomposite; coffee husk; magnesium iron oxide; acetaminophen

Introduction

Paracetamol (N-acetyl-para-aminophenol), denoted as PAR, is one of the most widely used analgesic and antipyretic agents worldwide [1,2]. It is widely used in clinical practice due to its effective analgesic properties and a favourable safety profile at therapeutic doses. However, paracetamol overdose can result in serious health complications, particularly hepatotoxicity, which may become life-threatening in severe cases [3-5]. Consequently, the development of accurate and reliable analytical methods for the quantification of paracetamol in biological and environmental samples is of critical importance [6].

In recent years, electrochemical techniques have gained prominence as efficient, rapid, and cost-effective tools for paracetamol detection [7]. These methods enable the determination of trace levels of the drug with high sensitivity and reduced analysis time [8]. The performance of electrochemical sensors is strongly influenced by the properties of electrode materials; thus, the design and development of novel electrode materials are essential for improving the sensitivity, selectivity, and overall analytical performance of these systems [8]. This study focuses on the development of a novel electrode composed of a nanocomposite of magnesium ferrite and activated carbon derived from coffee shells. Coffee shell, an abundant agricultural waste, is rich in carbon and other beneficial compounds, making it a valuable resource for material synthesis [9]. Utilizing activated carbon from coffee shell not only supports environmental sustainability by repurposing waste materials but also offers excellent properties for electrochemical applications. Owing to its high surface area, porosity, and conductivity, activated carbon is widely used in adsorption (Acda, 2014), catalysis, and electrochemical sensing [10].

In this context, integrating magnesium ferrite with coffee shell-derived activated carbon offers a promising approach to enhance the performance of electrochemical sensors. Magnesium ferrite (MF) is well known for its excellent electrochemical properties and strong catalytic activity, making it a promising material for sensor development [11]. When combined with activated carbon, the resulting composite benefits from a high surface area and enhanced electrical conductivity, two critical factors for improving the electrochemical sensitivity in paracetamol detection [12]. In this study, we employ electrochemical techniques such as voltammetry to determine paracetamol concentrations in test samples, thereby evaluating the performance of the newly developed electrode. We present the synthesis of a novel nanocomposite material composed of MF supported on activated carbon derived from coffee shell waste, prepared using a hydrothermal method. The work details the synthesis process, the electrochemical characterization techniques employed, and the results obtained, which contribute to the development of reliable and sensitive methods for PAR detection in pharmaceutical formulations.

Experimental

Materials and reagents

Coffee husks were collected from Dak Lak Province, crushed to a particle size of 0.1 to 0.5 mm, dried at 100 °C, and stored in a desiccator for further use. Magnesium chloride hexahydrate ($MgCl_2{\cdot}6H_2O$, 99 %, Merck) and iron(III) chloride hexahydrate ($FeCl_3{\cdot}6H_2O$, 98 %, Merck) were used as precursors for magnesium ferrite synthesis. Sodium hydroxide (NaOH, 99 %, Merck) served as the hydrolysis agent, while ethanol (C_2H_5OH, 99 %, Merck) was used as the solvent. Britton-Robinson (BR) buffer solution was prepared using ortho-boric acid (H_3BO_3, 99 %, Merck), ortho-phosphoric acid (H_3PO_4, 85 %, Merck), acetic acid (CH_3COOH, 99 %, Merck), and sodium hydroxide (NaOH,

99 %, Merck). Standard PAR was obtained from Merck, and commercial paracetamol tablets were purchased locally.

Preparation of magnesium ferrite/activated carbon from coffee husk

Coffee husks collected from Dak Lak Province were cleaned, dried, and soaked in a 1 M HNO_3 solution for 24 hours to remove residual metals. After acid treatment, the husks were thoroughly washed with distilled water until the pH was neutral, dried at 100 °C for 24 hours, and stored in a desiccator. The dried material was then placed in a nickel crucible with a lid and heated to 700 °C for 2 hours, yielding biochar (BIOC). To remove silica, 20 g of BIOC was treated with 200 mL of 0.5 M NaOH at 90 °C for 24 hours. The resulting mixture was washed repeatedly with distilled water, dried, and designated as silica-free biochar (BIOC-silica). Subsequently, 2 g of BIOC-silica was mixed with 2 g of NaOH in a nickel crucible, covered, and heated again at 700 °C for 2 hours. The product was then washed several times with distilled water to remove residual NaOH and dried at 100 °C for 24 hours, yielding the final activated carbon (AC) material. The synthesis of the $MgFe_2O_4$/activated carbon (MF/AC) nanocomposite was carried out based on a previously reported method with modifications. Specifically, 0.813 g of magnesium chloride hexahydrate ($MgCl_2{\cdot}6H_2O$), 2.163 g of iron(III) chloride hexahydrate ($FeCl_3{\cdot}6H_2O$), and 1.2 g of activated carbon (AC) derived from coffee husks were added to a 250 mL beaker containing 135 mL of distilled water. The mixture was stirred to ensure uniform dispersion. Separately, 1.280 g of sodium hydroxide (NaOH) was dissolved in 20 mL of distilled water and added dropwise to the mixture under continuous stirring for 15-20 minutes. The amount of NaOH was stoichiometrically calculated to react with 0.004 mol of Mg^{2+} and 0.008 mol of Fe^{3+} ions. The resulting mixture was transferred to a Teflon-lined stainless steel autoclave and subjected to hydrothermal treatment at 190 °C for 10 hours. After cooling to room temperature, the precipitate was collected, thoroughly washed with distilled water to remove residual ions, and dried. The final product was magnesium ferrite/activated carbon, labelled as MF/AC.

The ionic Equations (1) and (2) can represent the formation of $MgFe_2O_4$:

$$Mg^{2+} + 2Fe^{3+} + 8OH^- \rightarrow Mg(OH)_2\downarrow + 2Fe(OH)_3\downarrow \rightarrow MgFe_2O_4 + 4H_2O \quad (1)$$

$$MgFe_2O_4 + AC \rightarrow MgFe_2O_4/AC \quad (2)$$

Apparatus

Scanning electron microscopy (SEM) using a Nova NanoSEM 450 (USA) at the Vietnam Academy of Science and Technology was employed to investigate the surface morphology of the synthesized materials. Fourier transform infrared spectroscopy (FT-IR) was used to identify the functional groups present, utilizing an IR Affinity-1S spectrophotometer (Shimadzu) at Hue University, Vietnam. The crystalline structure of the materials was analysed using a Bruker D8 Advance X-ray diffractometer (Bruker, Germany), and energy-dispersive X-ray spectroscopy (EDX) was performed on a TEAM Apollo XL EDS system (USA) at the Vietnam Academy of Science and Technology. Additionally, nitrogen adsorption-desorption isotherms were used to determine the specific surface area and porosity *via* the Brunauer-Emmett-Teller (BET) method on a Micromeritics Tristar 3000 at the Vietnam Academy of Science and Technology. The magnetic properties were assessed using a Micro Sense Easy VSM 20130321-02 vibrating sample magnetometer (VSM) at Vietnam Academy of Science and Technology, and the optical bandgap energy was estimated using Ultraviolet-visible diffuse reflectance spectroscopy (UV-Vis DRS) with a UV-2600 Shimadzu (Japan) at Dong Thap University, Vietnam.

Preparation of glassy carbon electrode

Prior to modification, the bare glassy carbon electrode (GCE) was thoroughly polished using alumina slurry on sandpaper and rinsed multiple times with distilled water. The cleaned electrode was then dried at room temperature. To prepare the MF/AC suspension, 5 mg of the synthesized material was sonicated in 5 mL of distilled water for approximately three hours. Subsequently, 5 µL of the MF/AC suspension was drop-cast onto the polished GCE surface and dried in an oven at 40 °C for 12 hours to obtain the modified electrode ready for use.

A 0.01 M standard paracetamol (PAR) solution was prepared by accurately weighing the required amount and diluting to volume with deionized water. Britton-Robinson (BR) buffer solutions with pH values ranging from 2 to 8 were prepared by mixing 0.04 M boric acid, 0.04 M phosphoric acid, and 0.04 M acetic acid, and adjusting the pH with 0.2 M sodium hydroxide. All solutions were stored at 4 °C throughout the study.

Real sample preparation

Five units of each pharmaceutical formulation were weighed to determine the average tablet weight. A portion of the powdered sample, approximately 25 mg of PAR, was transferred to a 100 mL volumetric flask, dissolved in distilled water, and filtered. The resulting solution was then diluted tenfold for electrochemical analysis.

Electrochemical analysis

- **Sample testing:** an aliquot of 1 mL of the prepared solution was pipetted into an analytical cup, diluted with 0.1 M buffer solution (pH 7) to a final volume of 10 mL, and analysed under the optimized experimental conditions to quantify PAR in five pharmaceutical samples.
- **Recovery determination (spiked samples):** to assess accuracy, 1 mL of the prepared solution was mixed with 20 µL of 1 mM PAR standard, diluted with 0.1 M buffer solution (pH 7) to 10 mL, and analysed using the same optimized procedure. The recovery was calculated by comparing the detected and added amounts of PAR.

All electrochemical measurements were performed using a CPAHH5 electrochemical workstation (Vietnam) in a conventional three-electrode system. The setup consisted of a glassy carbon electrode (GCE, 2.8 mm diameter) as the working electrode, an Ag/AgCl electrode (Model RE-5, BAS) as the reference electrode, and a platinum wire as the counter electrode. Differential pulse voltammetry (DPV) was employed to quantitatively determine PAR in sample solutions using the standard addition method.

Results and discussion

Material characterization

The XRD analysis results are presented in Figure 1a. The XRD pattern of AC confirms that the activated carbon derived from the coffee husk is predominantly amorphous, with disordered graphitic domains. The presence of broad (002) and (100)/(101) peaks reflect incomplete graphitization. This structural disorder is beneficial for electrochemical applications, as it often correlates with a higher surface area and more active adsorption and electron-transfer sites. The XRD pattern of MF/AC contains peaks that match the standard data for the spinel phase $MgFe_2O_4$ with a cubic structure according to JCPDS No. 732410. The diffraction peaks at 2θ were obtained at 33.2, 35.6, 40.9, 49.2 and 54.0° indexed as (220), (311), (400) and (422). The XRD pattern of the MF/AC composite demonstrates the successful incorporation of crystalline $MgFe_2O_4$ nanoparticles onto the amorphous activated carbon

matrix. The coexistence of sharp ferrite peaks and broad carbon peaks confirms that the composite retains the distinct phases of both materials.

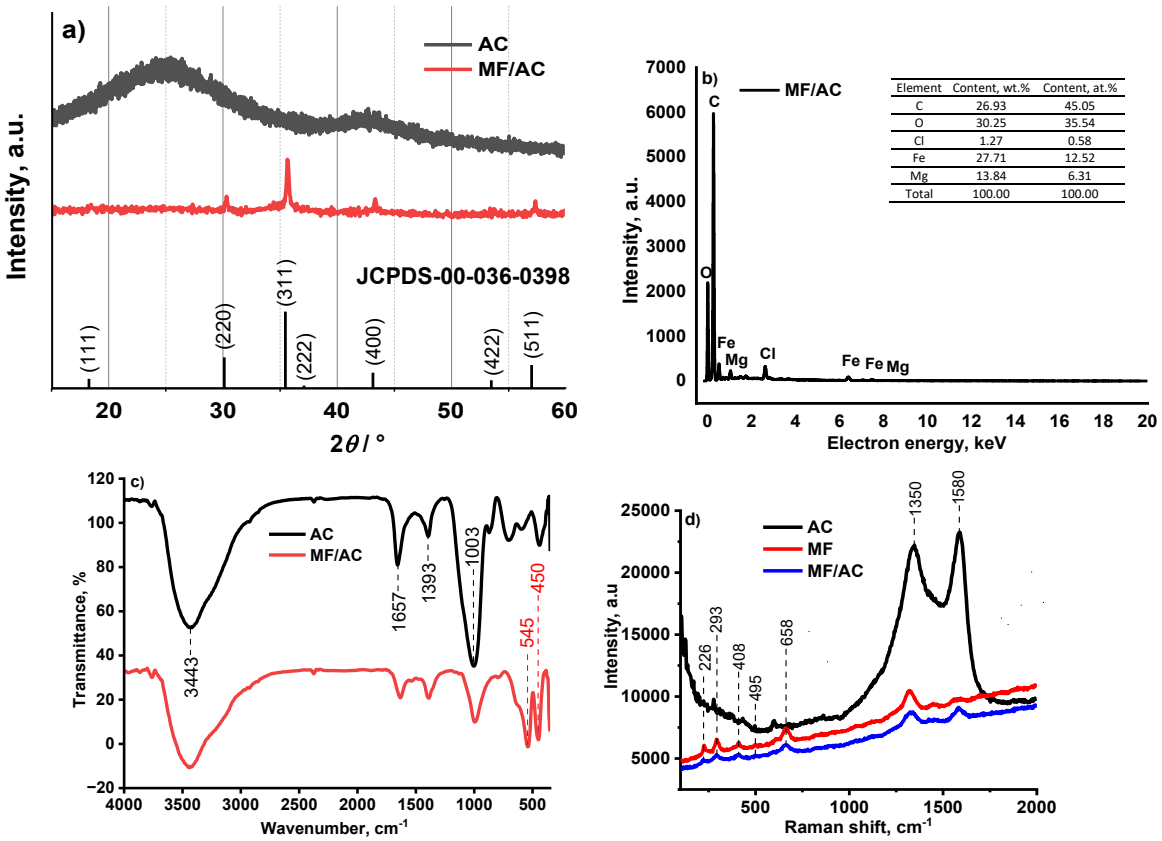

Figure 1. *a) XRD patterns of AC; b) EDX spectrum of MF/AC; c) FT-IR spectra and d) Raman spectra of AC, MF and MF/AC*

EDX analysis of the MF/AC composite (Figure 1b) detected Mg, Fe, O, and C, with Fe: Mg molar ratio of approximately 1.98. This molar ratio is very close to the theoretical stoichiometric ratio of 2:1 in MF, further confirming the successful synthesis. FTIR spectrum of AC (Figure 1c) shows a broad peak at 3443 cm^{-1} (O-H stretching), 1657 cm^{-1} (C=O vibrations), and peaks at 1393 and 1003 cm^{-1} (C-H or C-C groups). The characteristics of the activated carbon obtained in this study are similar to those found in several other studies [13,14]. For MF/AC, new bands at 545 and 450 cm^{-1}, assigned to Fe-O and Mg-O bonds in the $MgFe_2O_4$ spinel structure, respectively [15], confirming the integration of both components.

The Raman active modes of MF/AC were measured in the spectral range from 100 to 2000 cm^{-1} (Figure 1d). Five first-order Raman modes ($A_{1g} + E_g + 3F_{2g}$) appear under ambient conditions. For bulk ferrite, the modes above 600 cm^{-1} are mostly attributed to the movement of oxygen in the tetrahedral AO4 groups, with the mode at 657.45 cm^{-1} likely corresponding to the symmetric A_{1g} mode. Other low-frequency modes are characteristic of the octahedral site (BO6). The modes at 611.33, 453.05 and 215 cm^{-1} belong to the symmetric F_{2g}, while the mode at 306.32 cm^{-1} corresponds to the E_g symmetry. For iron-rich ferrite samples, the characteristic Raman bands of α-Fe_2O_3 appear at approximately 226.11, 292.63, 408.32 and 495 cm^{-1}, corresponding to A_{1g}, E_{1g}, E_{1g} and A_{1g}, respectively.

Figure 2a shows that AC is nonmagnetic, whereas the MF/AC material exhibits magnetic properties, with a maximum magnetization saturation (MS) of 3.0 A m^2 kg^{-1}. However, compared with previously reported values, this MF/AC material exhibits higher saturation magnetization. With negligible coercivity, no hysteresis loop appears on the magnetization curve of MF/AC, indicating that the synthesized material possesses a nanostructure with superparamagnetic properties.

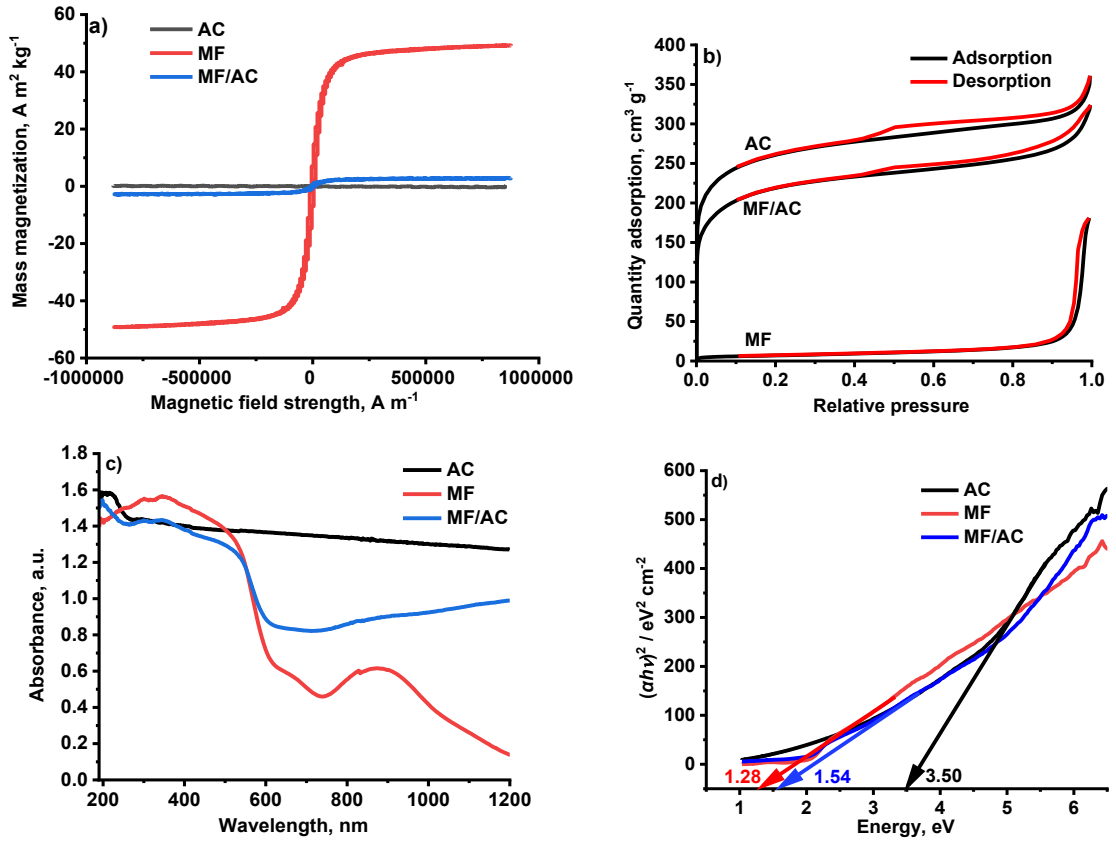

Figure 2. *a) Magnetic saturation curve, b) nitrogen adsorption/desorption isotherms, c) UV-Vis DRS spectra, and d) Tauc plots of AC, MF and MF/AC*

The textural properties of the obtained materials were studied using nitrogen adsorption/desorption isotherms (Figure 2b). It can be observed that these isotherms belong to type III according to the IUPAC classification. The results indicate that the specific surface areas calculated using the BET model for AC, MF, and MF/AC are 951.2, 24.5 and 788.7 $m^2 g^{-1}$, respectively. This demonstrates that the synthesized MF material exhibits a significant increase in specific surface area upon surface modification with activated carbon, suggesting that the MF/AC material has strong adsorption capacity for both small and bulky molecules.

Figures 2c and 2d show the UV-Vis DRS absorbance spectra of AC, MF, and the MF/AC composite, illustrating their optical absorption characteristics. The optical band gap was calculated using the Tauc equation, written as $(\alpha h\nu) = (Ah\nu - E_g)^n$, where E_g is the optical band gap, A is a constant, h is Planck's constant, ν is frequency, and n is an index that is typically considered to be two for direct allowed transitions, and 1/2 for indirect allowed transitions [16,17]. The calculated band structures of the normal spinel $MgFe_2O_4$ indicate that $MgFe_2O_4$ is a direct bandgap semiconductor [17]. Experimental optical studies typically assume a direct allowed transition [18,19]. Consequently, the optical bandgap energies, derived from the Tauc plots by extrapolating $(\alpha h\nu)^2$ versus $h\nu$, are 3.50 eV for AC, 1.28 eV for MF and 1.54 eV for MF/AC. These findings provide clear evidence for the successful formation of the MF/AC composite.

SEM images (Figure 3) show that the synthesized AC exhibits a relatively uniform morphology characterized by a rough surface and a large surface area (Figure 3a). MF particles are spherical, with diameters ranging from 50 to 100 nm and are homogeneously distributed (Figure 3b). In the MF/AC composite, these spherical particles are well dispersed on the AC surface, confirming successful formation (Figure 3c).

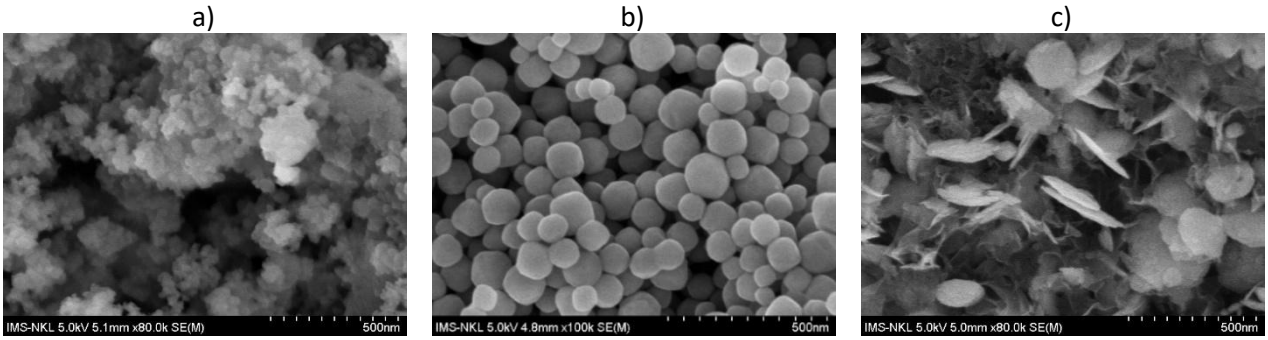

***Figure 3**. SEM images of a) AC, b) MF and c) MF/AC*

Electrochemical determination of paracetamol

Electrochemical response of the modified glassy carbon electrode to paracetamol

The electrochemical performance of different electrodes toward PAR detection was evaluated (Figure 4). The bare GCE exhibits the weakest redox response, while AC/GCE shows an improved current due to the higher surface area of activated carbon. The MF/GCE electrode further enhances the current response, demonstrating the electroactive contribution of MF. Notably, the MF/AC-GCE composite achieves the strongest redox response, confirming the synergistic effect of MF and AC in facilitating electron transfer. This trend is consistent with the bar graph in Figure 4b, where the current response follows the order: GCE (14.040 ± 0.467 µA) < AC/GCE (21.717 ± 0.643 µA) < < MF/GCE (25.875 ± 0.241 µA) < MF/AC-GCE (28.438 ± 0.670 µA).

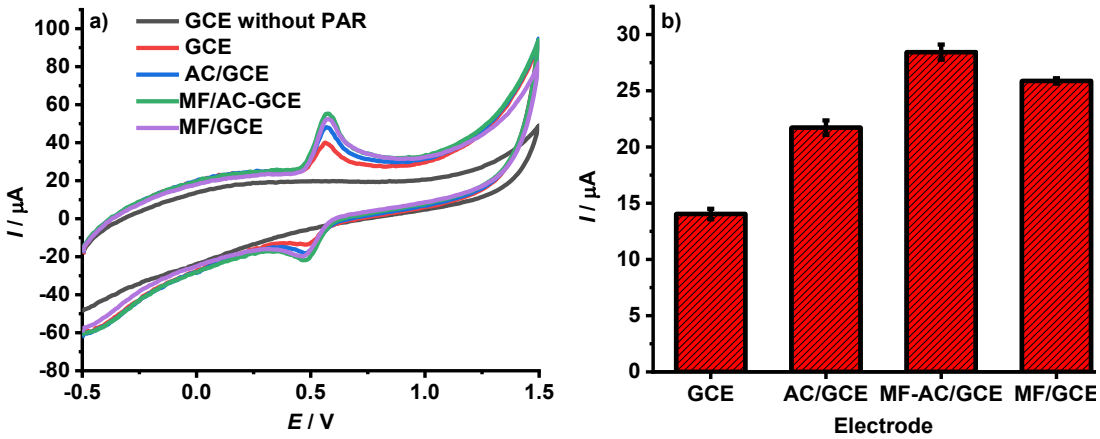

***Figure 4.** a) CV curves of PAR (C_{PAR} = 50 µM) at different electrodes in 0.1 M BRS, pH 5, scan rate v = 0.1 V s^{-1}; b) anodic peak currents at different electrodes*

The electrochemical behaviour of the electrodes was examined by measuring their effective electrochemical surface area (ECSA), as shown in Figure 5. The Randles-Ševčík equation was used to calculate ECSA [20]: $i_p = 2.69\times10^5\, n^{3/2} A D^{1/2} C\, v^{1/2}$, where i_p / A is peak current, A / cm² is ECSA, n is the number of electrons, D / cm² s^{-1} is diffusion coefficient, C / mol cm^{-3} is concentration and v / V s^{-1} is scan rate.

The bare GCE showed an ECSA of 0.040 cm², indicating the inherent activity of the unmodified carbon surface. After modification with activated carbon, the ECSA increased to 0.055 cm², indicating that the carbon material's porous microstructure and high surface area provided more electroactive sites and improved electrolyte access. Incorporating magnesium ferrite further raised the ECSA to 0.056 cm², likely due to the combined effect of its redox-active Fe^{2+}/Fe^{3+} couples, which help facilitate charge transfer at the electrode-electrolyte interface. Notably, the composite electrode with both

magnesium ferrite and activated carbon achieved the highest ECSA of 0.073 cm^2. This notable improvement shows a strong synergistic effect, where the conductive carbon network enhances electron transport. At the same time, the magnesium ferrite nanoparticles offer abundant catalytic sites, resulting in a more accessible and efficient electrochemical surface. Overall, the steady increase in ECSA indicates that combining activated carbon with magnesium ferrite is an effective strategy for maximizing the electrochemical performance of GCE-based sensors.

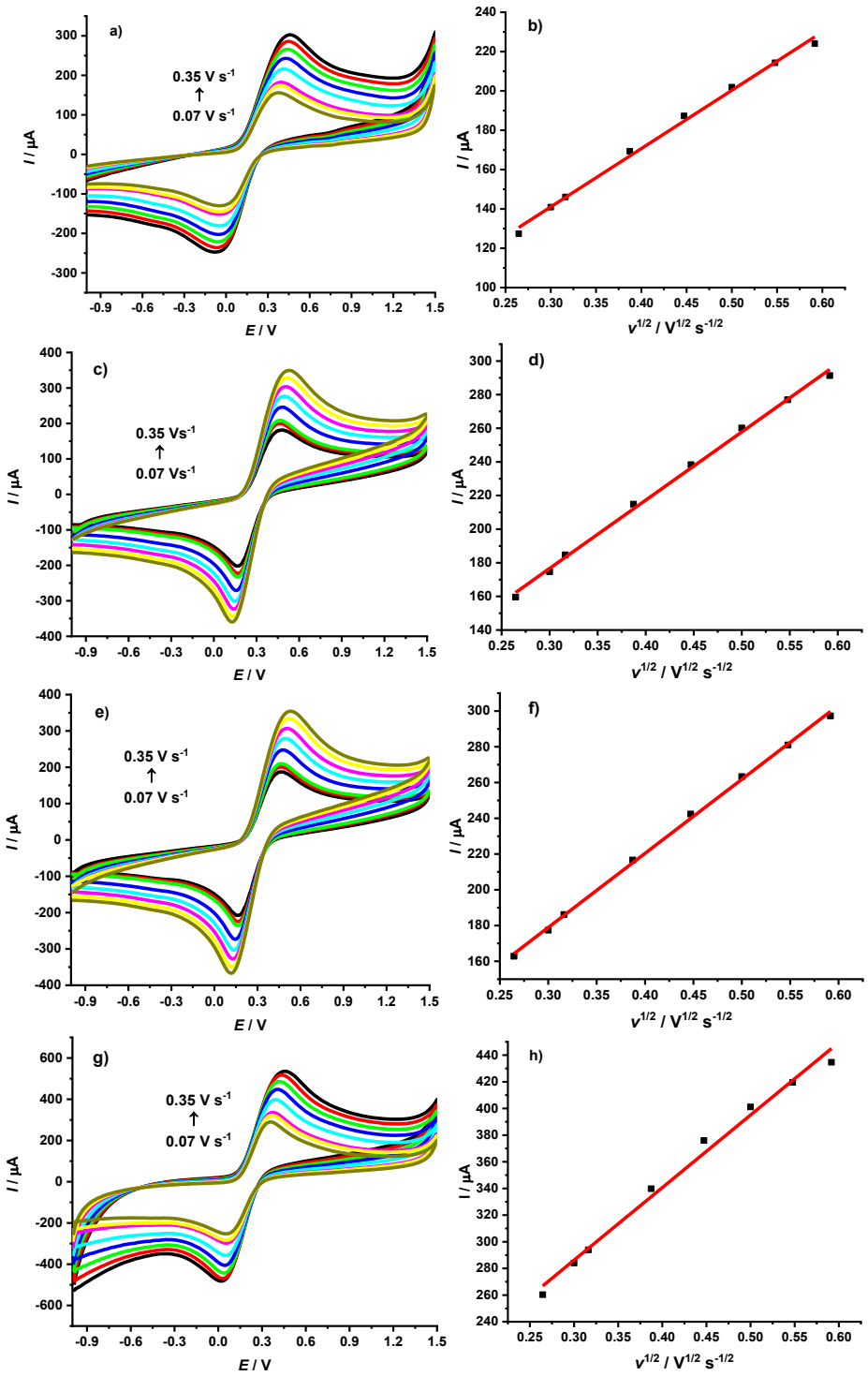

Figure 5. *Cyclic voltammograms of electrodes recorded in 0.1 M KCl containing 10 mM $[Fe(CN)6]^{3-/4-}$ at different scan rates (0.07 to 0.35 V s^{-1})(a, c, e and g) and corresponding linear relationships between the anodic peak current and the square root of the scan rate (b,d, g and h) at: bare GCE (a and b), AC/GCE (c and d, MF/AC (e and f) and MF/AC/GCE (g and h)*

The pH of the solution plays a crucial role in the electrochemical behaviour of PAR at the MF-AC/GCE-modified electrode. Figure 6a shows the CV curves of PAR at pH values ranging from 2 to 11. At pH values above 7, the peak current intensity decreases progressively with increasing pH. In contrast, at pH values below 7, the peak current generally increases with increasing pH, except at pH 5 (Figure 6b). The maximum peak current is observed at pH 7. Although the dependence of peak current intensity on pH is complex, the overall trend indicates a decrease at higher pH values. This behaviour may be attributed to the adsorption of PAR on the MF/AC/GCE surface. Because PAR contains aromatic rings and can undergo reduction, the electrode surface becomes negatively charged at high pH, thereby reducing analyte adsorption and decreasing current intensity. Based on both signal intensity and current stability, pH 7 was chosen for subsequent experiments.

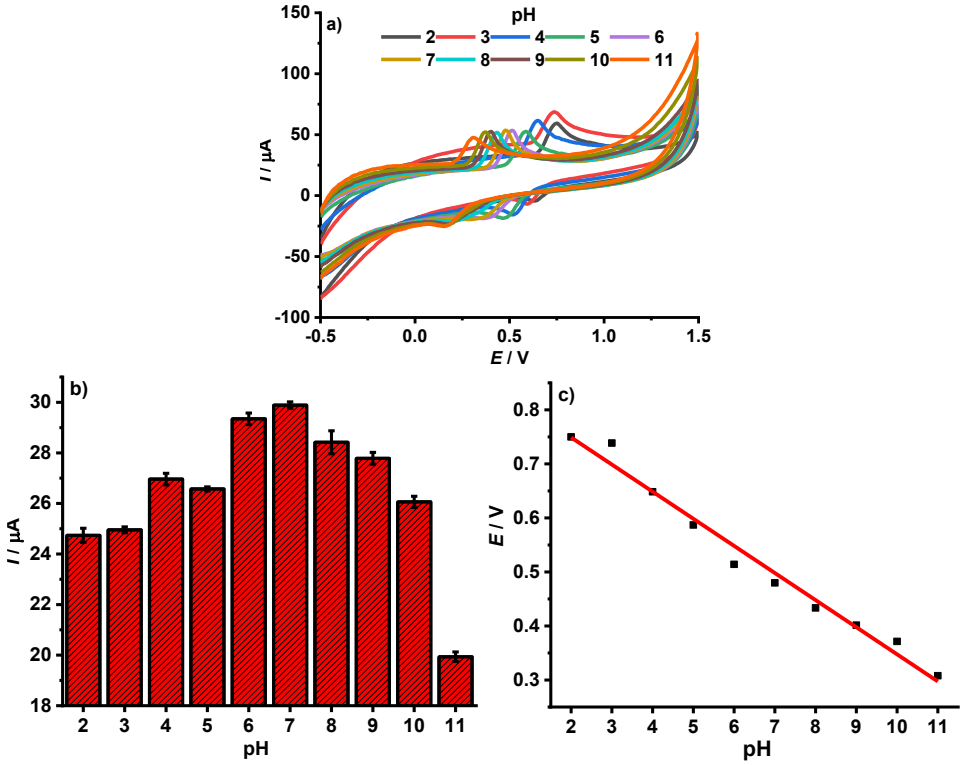

Figure 6. *a) CV curves of PAR (C_{PAR} = 50 µM) at MF/AC-GCE in 0.1 M BRS at pH 2-11, scan rate* v *= 0.1 V* s^{-1}*), b) effect of pH on the anodic peak current, c) linear plot of the peak potential (*E_p*)* vs. *pH*

In addition to affecting current intensity, pH also influences the oxidation peak potential (E_p) of PAR on the MF-AC/GCE electrode. As pH increases, the E_p value shifts negatively, and the relationship between E_p and pH is linear with a correlation coefficient of R^2 = 0.980 (Figure 6c). The regression Equation (3) is given as:

$$E_p = (0.849 \pm 0.018) + (-0.050 \pm 0.003)\ \text{pH}; \quad R^2 = 0.980 \qquad (3)$$

The slope of -0.052 V pH^{-1} is very close to the theoretical value of -0.059 V pH^{-1}, suggesting that the oxidation of PAR involves an equal number of electrons and protons.

The relationship between peak current and scan rate provides key insights into the mechanism of the electrochemical reaction. To investigate this, the effect of scan rate (v) on both peak current and peak potential was studied using cyclic voltammetry (Figure 7a). According to Soleymani *et al.* [21], a linear I_p - $v^{1/2}$ plot passing through the origin suggests a diffusion-controlled process, whereas a deviation from the origin indicates an adsorption-controlled process.

As shown in Figure 7 b, when the scan rate was varied from 50 to 400 mV s^{-1}, the oxidation peak current (I_p) of PAR exhibited a linear relationship with $v^{1/2}$, described by the regression Equation (4):

$$I_p = (2.312 \pm 1.141) + (86.082 \pm 2.577)\, v^{1/2}; \quad R^2 = 0.993 \tag{4}$$

Although the correlation coefficient indicates excellent linearity, the regression intercept is non-zero, indicating that the electrode process is primarily governed by adsorption rather than diffusion.

From the analysis of the graph depicting the relationship between I and $v^{1/2}$, it can be concluded that the adsorption process controls the oxidation of PAR at the MF-AC/GCE-modified electrode. This is characteristic of electrode processes in which the electrochemical reaction occurs prior to the corresponding chemical reaction.

Based on the Laviron Equation (5) [22], for a non-reversible system, the relationship between E_p and v is:

$$E_p = E^0 - \frac{RT}{(1-\alpha)nF}\ln\frac{RTK_S}{(1-\alpha)nF} + \frac{RT}{(1-\alpha)nF}\ln v \tag{5}$$

*wh*ere: E^0 is the standard electrode potential; α is the electron transfer coefficient; n is the number of exchanged electrons; F is Faraday's constant (96500 C mol^{-1}); K_s is the electron transfer rate constant; R and T are 8.314 J mol^{-1} K^{-1} and 298 K, respectively.

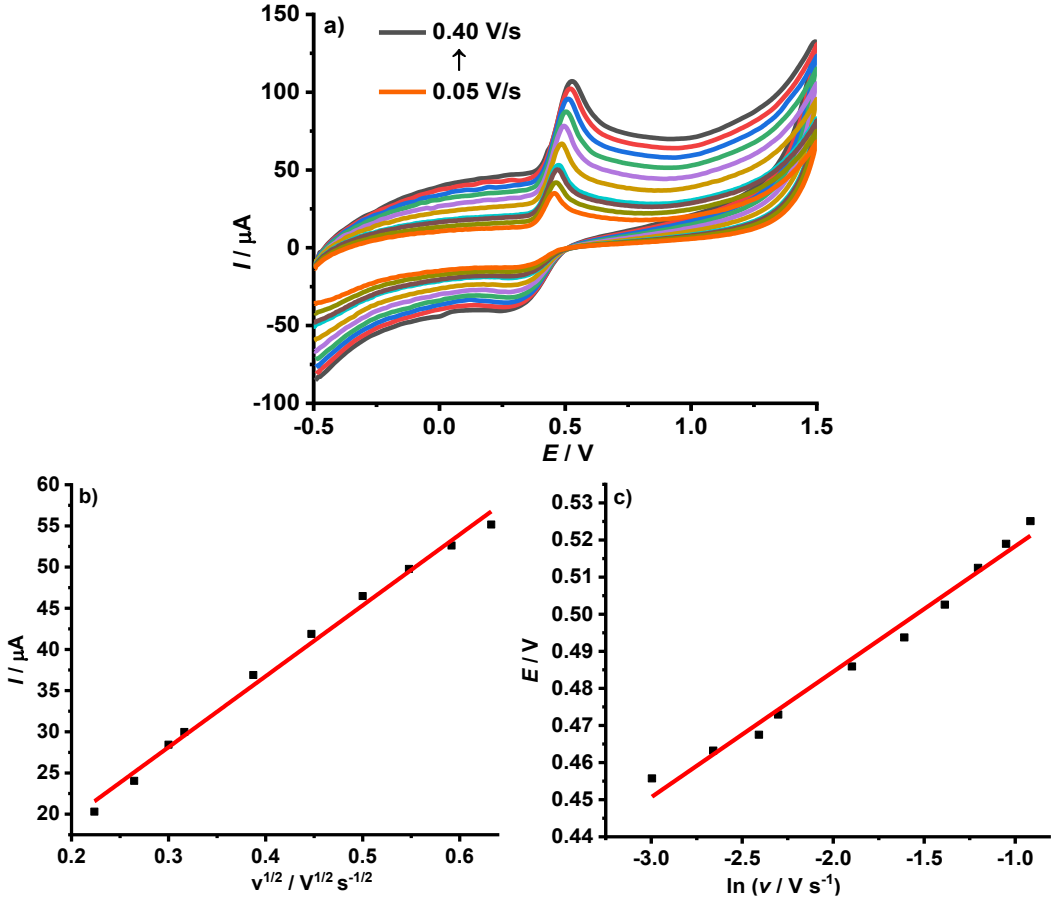

Figure 7. *a) CV curves of 50 µM PAR at MF/AC-GCE in 0.1 M BRS, pH 7, scan rate* ν *= 0.05 to 0.4 V* s^{-1}*; b) linear plot of peak current* vs. $\nu^{1/2}$*; c) linear plot of peak potential vs. ln v)*

In this study, the relationship between E_p and ln v for the oxidation of PAR is presented by Equation (6) (Figure 7c):

$$E_{p,PAR} = (0.552 \pm 0.003) + (0.034 \pm 0.002)\ln v; \; R^2 = 0.984 \tag{6}$$

Equation (6) shows a high linear correlation between E_p and ln v (R^2 = 0.984). From the slope of the straight line, the value of (1 - α) was obtained as 0.305, hence n is 0.695. For a non-reversible process, α is equal to 0.5 [23]. Therefore, the calculated value of n for PAR is approximately 1.6. Since n must be an integer, the value of n is 2. Thus, the redox process of PAR involves the transfer of 2 protons and 2 electrons.

The mechanism of PAR oxidation is shown in Scheme 1.

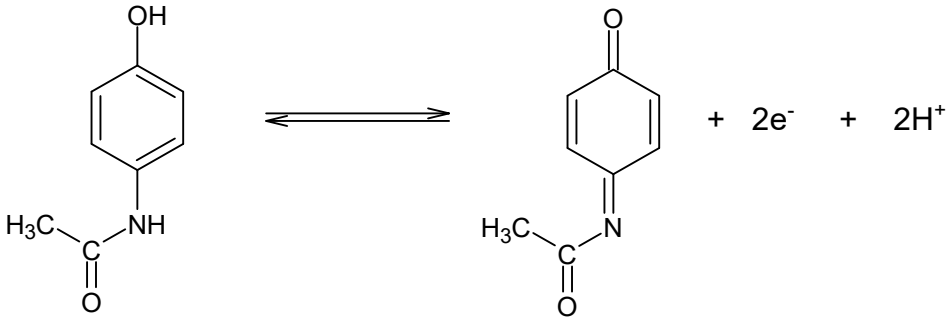

***Scheme 1**. The proposed mechanism of PAR oxidation at the MF/AC-GCE*

Optimizing the operational parameters

The study optimized several experimental parameters to achieve the clearest possible signal for PAR detection, including accumulation potential (E_{acc}), accumulation time (t_{acc}), pulse amplitude (E_{pulse}), and step voltage (E_{step}), as illustrated in Figures S1 to S4 (Supplementary Material). The optimal conditions were determined to be: E_{acc} = 0 V, t_{acc} = 15 s, E_{pulse} = 0.12 A, and E_{step} = 0.009 V.

Linearity and limit of detection for paracetamol

Under the optimized conditions, the PAR voltammetric response exhibits two distinct linear ranges: 1.0 to 9.9 µM (P1) and 9.9 to 47.62 µM (P2), as shown in Figure 8. The corresponding linear regression Equations (7) and (8) are:

Part 1: I_{PAR} = (3.1506±0.18494)+(2.71868±0.03004) C_{PAR}; R^2 = 0.99902; LOD_{PAR} = 0.29 µM (7)

Part 2: I_{PAR} = (24.11734±0.2136+(0.63684±0.00803) C_{PAR}; R^2 = 0.99873 (8)

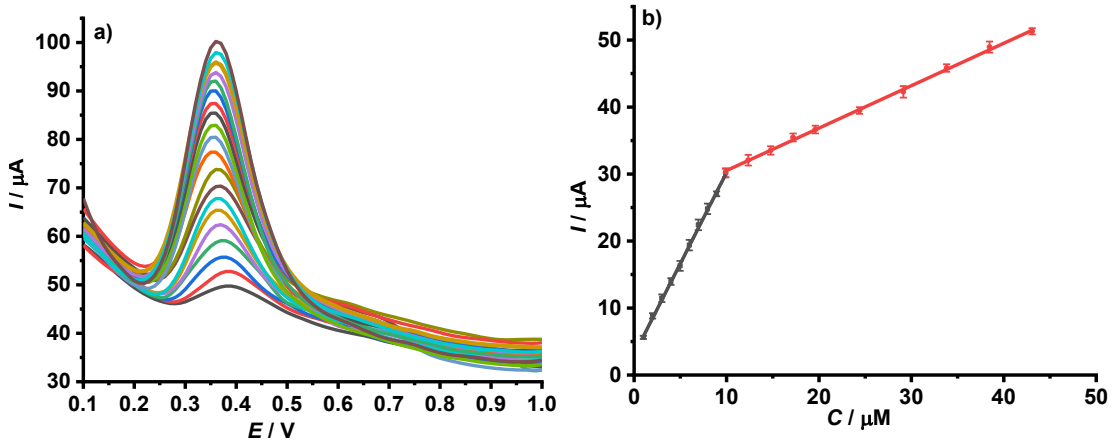

***Figure 8.** (a) Differential pulse voltammograms of PAR (1.0 to 47.62 µM) at MF/AC-GCE in 0.1 M BRS, pH 7 (conditions: scan rate 0.1 V s^{-1}, accumulation potential 0 V, accumulation time 15 s, pulse amplitude 0.12 A, step voltage 0.009 V); (b) plot of the peak current versus PAR concentration*

The calibration curve displays two linear segments because the electrochemical response of the analyte behaves differently at low and high concentrations. In the first segment (with a lower slope), the current is influenced by partial surface coverage, slow electron-transfer kinetics, or a combined

adsorption-diffusion process. As the analyte concentration increases, the system transitions to a diffusion-controlled regime in which the electrode's active sites are fully accessible, and the mass-transport rate accelerates. This dual-slope pattern is common in electroanalytical systems where reaction mechanisms, surface adsorption, or transport processes vary with concentration [24,25].

The calculated detection limit (LOD) of 0.29 μM is comparable to those reported for other electrochemical techniques for PAR determination. These findings demonstrate that the MF-AC/GCE-modified electrode provides a sensitive and reliable platform for PAR detection.

To contextualize the analytical performance of the proposed MF/AC sensor for paracetamol (PAR) determination, a comparative analysis with previously reported methods is essential. As summarized in Table 1, the sensor demonstrates competitive performance with other previously reported electrodes [26-33]. The LOD of our method (0.29 μM) is higher than that of unmodified electrodes, such as the GCE (0.369 μM) [27], and other modified sensors, including the molecularly imprinted polymer-modified pencil graphite electrode (MIP-PGE) (0.79 μM) [29]. While several advanced methods, such as those utilizing OP-PGE [30], $(MWCNTs\text{-}G4.0)_6$/GCE [31], PDTTP/PGE [32] and MIP/PB/GCE [33] report lower detection limits, they often present significant trade-offs. Specifically, some of these highly sensitive approaches are characterized by "tedious and multistep electrode preparation steps, and long analysis times". For instance, the oxidative pretreated pencil graphite electrode (OP-PGE) achieves an impressive LOD of 0.0148 μM [30], but its fabrication protocol is hazardous, requiring the electrode to be "boiled in nitric acid for 90 min at 115 °C". In this context, the MF/AC sensor emerges as an optimized and pragmatic solution, effectively bridging the gap between simple, less sensitive methods and complex, ultrasensitive ones. It provides sufficient sensitivity for pharmaceutical analysis while maintaining a fabrication process that is comparatively straightforward, safe, and cost-effective. This combination makes the MF/AC sensor a promising tool for routine analysis and quality control applications, where efficiency, reliability, and practical feasibility are paramount.

Table 1. *Comparison of analytical performance of the proposed MF/AC sensor with previously reported electrodes for PAR detection*

Electrode	Method	Linear range, μM	LOD, μM	Sample matrix	Ref.
Cu(II)-DPM/DDT modified gold electrode	OSWV	0.02 to 1500	120	Pharmaceutical samples	[26]
GCE	DPV	4 to 100	0.369	Tablet dosage forms	[27]
MWCNTs/poly(Gly) modified GCE	DPV	0.5 to10	0.5	Pharmaceutical samples	[28]
MIP-PGE	DPV	5 to 500 1250 to 4500	0.79	Commercial pharmace-utical tablets and syrup	[29]
OP-PGE	AdSWV	0.052 to 2.85	0.0148	Pharmaceutical tablets	[30]
$(MWCNTs\text{-}G4.0)_6$/GCE	DPV	0.3 to 200	0.1	Pharmaceutical samples	[31]
PDTTP/PGE	DPV	0.025 to 5	0.00194	Pharmaceuticals	[32]
MIP/PB/GCE	DPV	0.0001 to 1.0	0.00053	Pharmaceutical samples	[33]
MF/AC	DPV	1.0 to 9.9 9.9 to 47.62	0.29	Pharmaceutical samples	This work

Cu(II)-DPM: Dipyrromethene-Cu(II); MIP: molecularly imprinted polypyrrole; MWCNTs/poly(Gly): multi-walled carbon nanotubes/poly(glycine); GCE: glassy carbon electrode; OP-PGE: oxidative pretreated pencil graphite electrode; $(MWCNTs\text{-}G4.0)_6$: multiwalled carbon nanotubes (MWCNTs) and the fourth generation poly(amidoamine) dendrimers; PDTTP: Poly[2,5-di(2-Thiophenyl)-1-p-(Tolyl)Pyrrole]; MIP/PB: Prussian blue/layer of molecularly imprinted polypyrrole

Repeatability, reproducibility and long-term stability

The repeatability of peak current on the MF/AC-GCE electrode is evaluated by comparing the relative standard deviation (RSD) with the RSD calculated using the Horwitz equation: $RSD_H = 21 - 0.5 \log C$, where C is the molar concentration (Table 2 and Figure 9). Acceptable repeatability is defined as RSD being less than half of RSD_H. Each peak current value was measured

10 times at three different PAR concentrations (5, 10 and 20 µM). The RSD values are below the respective half-RSD_H values, indicating good repeatability for all measurements. Therefore, the modified MF-AC/GCE electrode can be used multiple times to determine PAR, even at low or high concentrations.

Table 2. *Average values of I, RSD and ½RSD_H for PAR determination*

	C_{PAR} / µM	$I_{average}$ / µA	SD	RSD, %	½RSD_H, %
Experiment 1	50	17.45	0.45	2.59	4.44
Experiment 2	100	30.12	0.45	1.49	4.00
Experiment 3	200	37.37	0.90	2.41	3.60

SD: standard deviation; RSD: relative standard deviation; *n = 10*

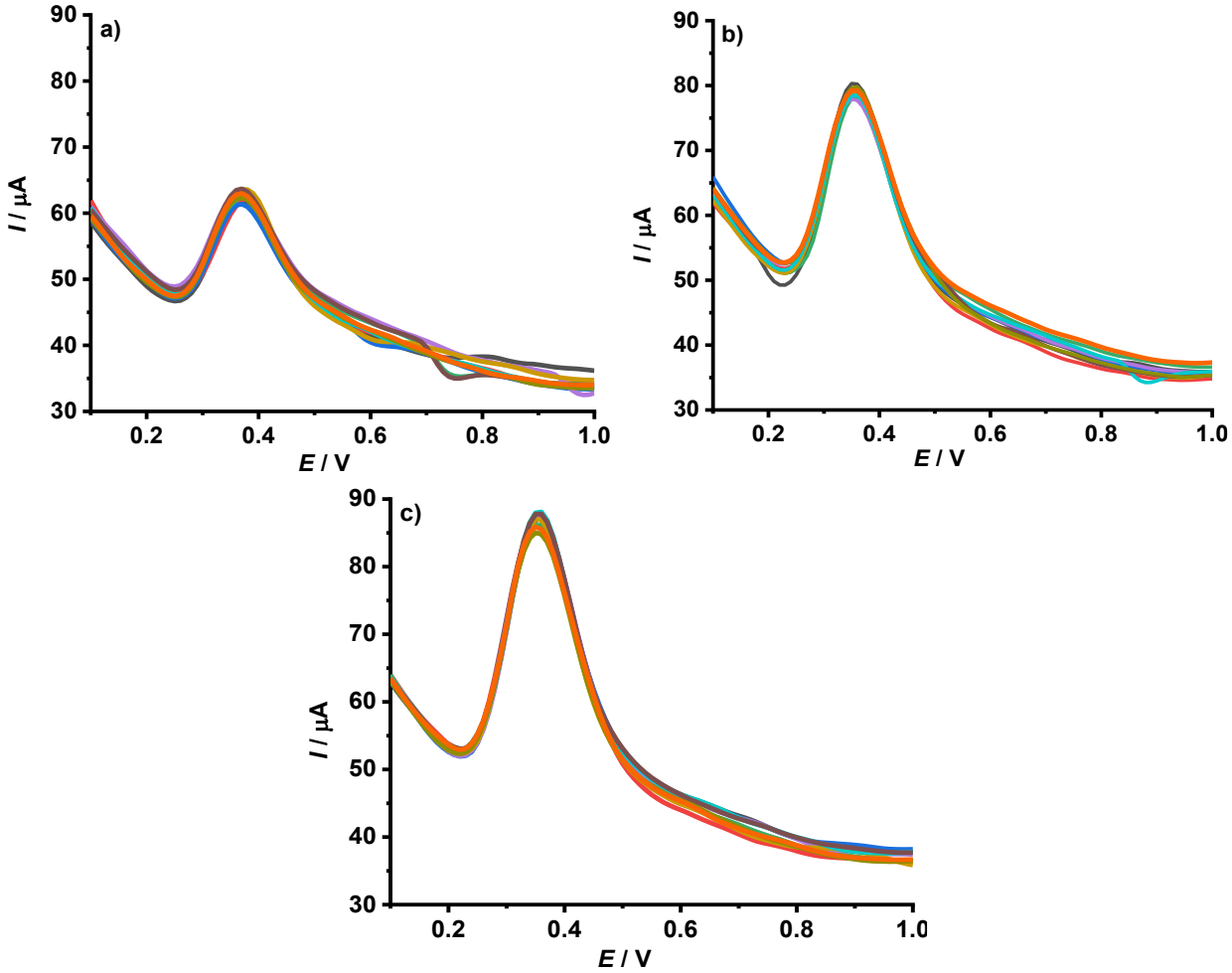

Figure 9. *DPV curves of the same MF/AC-GCE at three concentrations of PAR: a) 5 µM, b) 10 µM, c) 20 µM in 0.1 M BRS buffer, pH 7*

Repeatability is a key factor in assessing the method's accuracy. Under optimized conditions, DPV measurements were performed using nine independently fabricated MF/AC-GCEs. The maximum peak current response showed no significant variation among electrodes, with the relative standard deviation (RSD, n = 9) calculated as 4.24 % (I_{par} = 27.82 ± 1.18 µA) (Figure 10a).

The long-term stability of the electrode was evaluated by storing it at +4 °C under humid conditions. The electrode response was tested daily in a 5 µM PAR solution prepared in 0.1 M BRS buffer (pH 7) over nine days. The average peak current after this period was I_{par} = 25.39 ± 0.22 µA, corresponding to an RSD of 0.86 %, confirming excellent stability (Figure 10b).

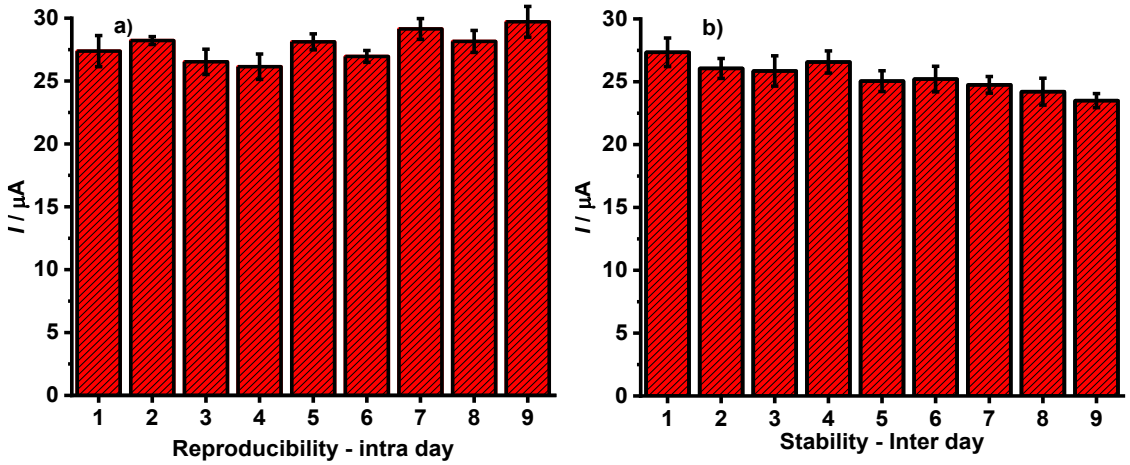

Figure 10. *Peak current I_p for C_{PAR} = 10 µM in 0.1 M BRS buffer, pH 7 for: a) nine times prepared MF/AC-GCE using the same procedure; b) nine-day long-term stability*

Interference study

The selectivity of the modified electrode was examined in the presence of 12 potential interfering substances at a PAR concentration of 20 µmol L^{-1}. The tolerance limit was defined as the maximum concentration of an interfering species that causes a relative error of about 5 % in the PAR signal. As summarized in Table 3, the results demonstrated that up to 100-fold higher concentrations of $AlCl_3$, NH_4Cl, NH_4NO_3, D-glucose, L-cysteine, and D-sucrose, 80-fold higher concentrations of Na_2SO_4, $Ca(HPO_4)_2$, KNO_3, caffeine, and glutamic acid, and 60-fold higher concentrations of sodium benzoate did not significantly affect the peak current of PAR. These findings confirm that the proposed method exhibits excellent selectivity and is suitable for reliable PAR detection in real samples.

Table 3. *Influence of some interfering substances on the peak current intensity of PAR at MF/AC-GCE*

Number	Substance	$C_{substance}$ / C_{PAR}	I_p / µA)	Re, %
1	$AlCl_3$	100	40.58	3.72
2	Na_2SO_4	80	37.88	-3.93
3	NH_4Cl	100	37.37	-3.98
4	NH_4NO_3	100	37.37	-3.98
5	$Ca(HPO_4)_2$	80	38.49	-2.90
6	KNO_3	80	37.95	-4.99
7	Caffeine	80	39.48	-2.92
8	D-Glucose	100	40.20	-3.50
9	Sodium benzoate	60	36.65	4.31
10	L-Cysteine	100	40.34	4.66
11	D-sucrose	100	38.92	-3.68
12	Glutamic acid	80	40.61	-4.15

Analytical application of the proposed DPV method to real samples

The determination of PAR in pharmaceutical samples was carried out using DPV with an MF/AC-GCE modified electrode. The results summarized in Table 4, showed recovery values ranging from 96.09 to 104.01 %. These results demonstrate both the accuracy and reliability of the proposed method for real-sample analysis. Therefore, the MF/AC-GCE-based method is a promising approach for the determination of PAR in pharmaceutical formulations.

The quantification of PAR in pharmaceutical formulations was carried out using the standard addition method. Each sample was analysed in triplicate under identical experimental conditions. The recovery rates of PAR in real samples were calculated to evaluate the accuracy of the proposed method. After the known amounts of PAR were added, the compounds were reanalysed using the

standard addition procedure. The recovery values ranged from 96.09 to 104.01 %**,** confirming the reliability of the method.

Table 4. *Results of PAR analysis in pharmaceutical samples*

Sample	Amount of PAR on the label, mg *per* tablet	Amount of PAR analysed, mg		Amount of PAR, µg		Recovery, %
		HPLC	DPV	Added	Found ± SD	
Hapacol 80	80	81.8 ± 0.9	80.1 ± 0.9	3.0233	3.1446 ± 0.0860	104.01
Hapacol 150	150	148.8 ± 0.8	153.4 ± 4.4	3.0233	3.1034 ± 0.0944	102.65
Hapacol 250	250	249.0 ± 1.3	244.5 ± 2.4	3.0233	2.9051 ± 0.1238	96.09
Partamol tab.	500	487.9 ± 0.7	492.0 ± 5.1	3.0233	2.9940 ± 0.0298	99.03
Hapacol 650	650	640.8 ± 0.9	643.8 ± 2.7	3.0233	3.0910 ± 0.1046	102.24

For validation, PAR was also quantified using high-performance liquid chromatography (HPLC)**.** The results obtained by both methods were highly consistent. A paired *t*-test was performed, yielding a calculated *t* value of 1.362, which is lower than the critical value of 2.78. This indicates that there is no significant difference between the proposed electrochemical method and the HPLC reference method.

These findings demonstrate that the MF-AC/GCE-modified electrode is a reliable and accurate platform for the determination of PAR in pharmaceutical samples, with strong potential for practical applications.

Conclusion

A novel composite material, magnesium ferrite on an activated carbon substrate derived from coffee shells, has been successfully synthesized and characterized. The modified MF/AC electrode demonstrated excellent performance for the electrochemical determination of paracetamol. Under optimal conditions (pH 7), the sensor exhibited high sensitivity with a low detection limit (0.29 µM), good stability, and high selectivity. The method was successfully applied to analyse PAR in five commercial pharmaceutical formulations, with recovery rates ranging from 96.09% to 104.01%. The results showed strong agreement with the standard HPLC method, confirming the accuracy and reliability of the proposed sensor for practical applications in pharmaceutical quality control.

Supplementary material

Additional data are available at *https://pub.iapchem.org/ojs/index.php/JESE/article/view/3048* or from the corresponding author upon request.

Funding: *This research was supported by Hue University under the Core Research Program No. NCTB.DHH.2025.05.*

Conflict of interest: *The authors declare no conflict of interest.*

Author contributions: *Study conception and design: P.T.K.T, D.Q.K.; data collection: N.M.T, N.Q.M, N.H.P, P.T.Q; analysis and interpretation of results: P.T.K.T, D.Q.K. The first draft of the manuscript was written by P.T.K.T and D.Q.K. and all authors commented on previous versions of the manuscript. All authors read and approved the final manuscript.*

References

[1] M. Jozwiak-Bebenista, J. Nowak, Paracetamol: Mechanism of Action, Applications and Safety Concern, *Acta Poloniae Pharmaceutica* **71 (1)** (2014) 11-23. https://www.ptfarm.pl/pub/File/Acta_Poloniae/2014/1/011.pdf

[2] M. de Martino, A. Chiarugi, Recent Advances in Pediatric Use of Oral Paracetamol in Fever and Pain Management, *Pain and Therapy* **4** (2015) 149-168. https://dx.doi.org/10.1007/s40122-015-0040-z

[3] K. Du, A. Ramachandran, H. Jaeschke, Oxidative stress during acetaminophen hepatotoxicity: Sources, pathophysiological role and therapeutic potential, *Redox Biology* **10** (2016) 148-156. https://dx.doi.org/10.1016/j.redox.2016.10.001
[4] H. Jaeschke, M. McGill, C. Williams, A. Ramachandran. Current issues with acetaminophen hepatotoxicity-A clinically relevant model to test the efficacy of natural products, *Life Sciences* **88** (2011) 737-745. https://dx.doi.org/10.1016/j.lfs.2011.01.025
[5] M. Olaleye, B. Rocha, Acetaminophen-induced liver damage in mice: Effects of some medicinal plants on the oxidative defense system, *Experimental and Toxicologic Pathology* **59** (2008) 319-327. https://dx.doi.org/10.1016/j.etp.2007.10.003
[6] C. Fernandez, Z. Heger, R. Kizek, T. Ramakrishnappa, A. Borun, N. Faisal, Pharmaceutical Electrochemistry: The Electrochemical Oxidation of Paracetamol and Its Voltammetric Sensing in Biological Samples Based on Screen Printed Graphene Electrodes, *International Journal of Electrochemical Science* **10** (2015) 7440-7452. https://dx.doi.org/10.1016/S1452-3981(23)17361-5
[7] S. B. J. Shashikumara, Electrochemical investigation of dopamine in presence of Uric acid and ascorbic acid at poly (Reactive Blue) modified carbon paste electrode. A voltammetric study, *Sensors International* **1** (2020) 100008. https://dx.doi.org/10.1016/j.sintl.2020.100008
[8] Y. Nikodimos, M. Amare, Electrochemical determination of metronidazole in tablet samples using carbon paste electrode, *Journal of Analytical Methods in Chemistry* (2016) 361294. https://dx.doi.org/10.1155/2016/3612943
[9] M. N. Acda, E. E. Devera, Physico-Chemical Properties of Wood from Forest Residues. *Journal of Tropical Forest Science* **26** (2014) 589-595. https://www.jstor.org/stable/43150945
[10] R. Wulandari, A. Ardiansyah, H. Setiyanto, V. Saraswaty, A novel non-enzymatic electrochemical uric acid sensing method based on nanohydroxyapatite from eggshell biowaste immobilized on a zinc oxide nanoparticle modified activated carbon electrode. *RSC Advances* **13** (2023) 12654-12662. https://dx.doi.org/10.1039/D3RA01214J
[11] R. M. Khafagy, Synthesis, characterization, magnetic and electrical properties of the novel conductive and magnetic Polyaniline/MgFe2O4 nanocomposite having the core-shell structure, *Journal of Alloys and Compounds* **509** (2011) 9849-9857. https://dx.doi.org/10.1016/j.jallcom.2011.07.008
[12] R. S. Salama, M. S. Gouda, M. F. A. Aboud, F. T. Alshorifi, A. A. El-Hallag, A. K. Badawi. Synthesis and characterization of magnesium ferrite-activated carbon composites derived from orange peels for enhanced supercapacitor performance, *Scientific Reports* **14** (2024) 8223. https://dx.doi.org/10.1038/s41598-024-54942-9
[13] W. Li, J. Peng, L. Zhang, K. Yang, H. Xia, S. Zhang, S. Guo, Preparation of activated carbon from coconut shell chars in pilot-scale microwave heating equipment at 60 kW, *Waste Management* **29** (2009) 756-760. https://dx.doi.org/10.1016/j.wasman.2008.03.004
[14] T. Zhang, W. P. Walawender, L. T. Fan, M. Fan, D. Daugaard, R. C. Brown, Preparation of activated carbon from forest and agricultural residues through CO_2 activation, *Chemical Engineering Journal* **105** (2005) 53-59. https://dx.doi.org/10.1016/j.cej.2004.06.011
[15] A. Pradeep, P. Priyadharsini, G. Chandrasekaran, Sol- gel route of synthesis of nanoparticles of $MgFe_2O_4$ and XRD, FTIR and VSM study, *Journal of Magnestism and Magnetic Materials* **320** (2008) 2774-2779. https://dx.doi.org/10.1016/j.jmmm.2008.06.012
[16] J. Tauc, Optical properties and electronic structure of amorphous Ge and Si, *Materials Research Bulletin* **3** (1968) 37-46. https://dx.doi.org/10.1016/0025-5408(68)90023-8
[17] H. H. Kora, M. Taha, A. Abdelwahab, A.A. Farghali, S.I. El-dek, Effect of pressure on the geometric, electronic structure, elastic, and optical properties of the normal spinel $MgFe_2O_4$: a first-principles study, *Materials Research Express* **7** (2020) 106101. https://dx.doi.org/10.1088/2053-1591/abc049

[18] A.M. El-Khawaga, M. MohamedAyman, O. Hafez, R.E. Shalaby, Photocatalytic, antimicrobial and antibiofilm activities of $MgFe_2O_4$ magnetic nanoparticles, *Scientific Reports* **14** (2024) 12877. https://doi.org/10.1038/s41598-024-62868-5

[19] R. Srimathi, N.V.S.S. Seshagiri Rao, A. Merlin, R. Kiruthika, A. Selvaraj, O.H. Abdelkader, C.S. Dash, S. Revathi, A. Ahamed, J.R. Rajabathar, M. Sundararajan, S. Yuvaraj, L. Rajadurai, Investigation of structural, magnetic, optical and dielectric characteristics of Al-doped $MgFe_2O_4$ nanoparticles, *Solid State Sciences* **159** (2025) 107761. https://doi.org/10.1016/j.solidstatesciences.2024.107761

[20] A.J. Bard, L.R. Faulkner, *Electrochemical Methods: Fundamentals and Applications (2nd ed.),* John Wiley & Sons, 2001. ISBN 978-1-118-31280-3

[21] J. Soleymani, M. Hasanzadeh, N. Shadjou, M. K. Jafari, J. V. Gharamaleki, M. Yadollahi. A. Jouyban, A new kinetic-mechanistic approach to elucidate electrooxidation of doxorubicin hydrochloride in unprocessed human fluids using magnetic graphene based nanocomposite modified glassy carbon electrode, *Material Science Engineering C* **61** (2016) 638-650. https://dx.doi.org/10.1016/j.msec.2016.01.003

[22] E. Laviron, General expression of the linear potential sweep voltammogram in the case of diffusionless electrochemical systems, *Journal of Electroanalytical Chemistry and Interfacial Electrochemistry* **101** (1979) 19-28. https://dx.doi.org/10.1016/S0022-0728(79)80075-3

[23] C. Li, Electrochemical determination of dipyridamole at a carbon paste electrode using cetyltrimethyl ammonium bromide as enhancing element, *Colloids and Surfaces B* **55** (2007) 77-83. https://dx.doi.org/10.1016/j.colsurfb.2006.11.009

[24] D. Jemmelia, N. Fourati, H. B. Nacef, M. Dammak, C. Mousty, C. Gondran, E. D. Darii, Development of a new bisphenol A electrochemical sensor based on a cadmium(II) porphyrin modified carbon paste electrode, *RSC Advances* **10** (2020) 29399-29409. https://dx.doi.org/10.1039/D0RA04793G

[25] T. D. Doan, H. T. Nguyen, T. T. Tran, T. K. H. Dinh, M. H. Ha, T. T. L. Ho, N. T. Tran, T. O. Vu, T. H. Nguyen, T. L. Le, D. D. Le, N. P. Doan, Y. H. Tran, A highly sensitive electrochemical sensor for the detection of lead(II) ions utilizing rice-shaped bimetallic MOFs incorporated reduced graphene oxide, *RSC Advances* **15** (2025) 5356-5368. https://dx.doi.org/10.1039/D4RA08215A

[26] B. Saraswathyamma. I. Grzybowska, C. Orlewska, J. Radecki, W. Dehaen, K. G. Kumar, H. Radecka, Electroactive dipyrromethene-Cu(II) monolayers deposited onto gold electrodes for voltammetric determination of paracetamol, *Electroanalysis* **20** (2008) 2317-2323. https://dx.doi.org/10.1002/elan.200804328

[27] C. Engin, S. Yilmaz, G. Saglikoglu, S. Yagmur, M. Sadikoglu, Electroanalytical Investigation of Paracetamol on Glassy Carbon Electrode by Voltammetry, *International Journal of Electrochemical Science* **10** (2015) 1916-1925. https://dx.doi.org/10.1016/S1452-3981(23)05122-2

[28] P. V. Narayana, T. M. Reddy, P. Gopal, G. R. Naidu, Electrochemical sensing of paracetamol and its simultaneous resolution in the presence of dopamine and folic acid at a multi-walled carbon nanotubes/poly(glycine) composite modified electrode, *Analytical Methods* **6** (2014) 9459-9468. https://dx.doi.org/10.1039/C4AY02068E

[29] L. Özcan, Y. Şahin, Determination of paracetamol based on electropolymerized-molecularly imprinted polypyrrole modified pencil graphite electrode, *Sensors and Actuators Bl* **127** (2007) 362-369. https://dx.doi.org/10.1016/j.snb.2007.04.034

[30] E. Keskin, A. S. Ertürk, Electrochemical determination of paracetamol in pharmaceutical tablet by a novel oxidative pretreated pencil graphite electrode, *Ionics* **24** (2018) 4043-4054. https://dx.doi.org/10.1007/s11581-018-2532-4

[31] Y. Zhang, X. Liu, L. Li, Z. Guo, Z. Xue, X. Lu, An electrochemical paracetamol sensor based on layer-by-layer covalent attachment of MWCNTs and a G4.0 PAMAM modified GCE, *Analytical Methods* **8** (2016) 2218-2225. https://dx.doi.org/10.1039/c5ay03241e

[32] H. Gorcay, I. Celik, E. Yurdakul, Y. Sahin, S. Kokten, Highly sensitive electrochemical determination of acetaminophen in pharmaceuticals by poly[2, 5-di(2-Thiophenyl)-1-p-(Tolyl)Pyrrole] modified pencil graphite electrode, *IEEE Sensors Journal* **16** (2016) 2914-2921. https://dx.doi.org/10.1109/JSEN.2016.2526609

[33] Y. Dai, X. Li, X. Lu, X. Kan, Voltammetric determination of paracetamol using a glassy carbon electrode modified with Prussian blue and a molecularly imprinted polymer, and ratiometric read-out of two signals, *Microchimica Acta* **183** (2016) 2771-2778. https://dx.doi.org/10.1007/s00604-016-1926-0